Article n°3

Sommaire

1- Page de garde du journal mentionnant la ou les bases de son indexation ou le numéro d'identification ISSN
https://www.springer.com/journal/10948

2- L'abstract de l'article ou toutes informations référencées par la base de données d'indexation (preuves d'indexation)

- **https://www.scopus.com/sourceid/5100154501**
- **https://cassi.cas.org/publication.jsp?P=LglBQf5Q2NQyz133K_ll3zLPXfcr-WXfS7HRxbqcZSZujlCaOH557zLPXfcr-WXfimSBIkq8XcUjhmk0WtYxmzLPXfcr-WXfSPYhvXXuopikdxzQwzaXnA**
- **https://www.scimagojr.com/journalsearch.php?q=5100154501&tip=sid**

3- Tiré-à-part de l'article
https://doi.org/10.1007/s10948-018-4876-4

1- Page de garde du journal mentionnant la ou les bases de son indexation ou le numéro d’identification ISSN

Journal of Superconductivity and Novel Magnetism

The Journal of Superconductivity and Novel Magnetism serves as the international forum for the most current research and ideas in these fields. This highly acclaimed journal publishes peer-reviewed original papers, conference proceedings and review articles examining all aspects of the science and technology of superconductivity, including new materials, new mechanisms, basic and technological properties, new phenomena, and small- and large-scale applications. The rapidly expanding field of novel magnetism is also featured in the journal. Coverage focuses on such topics as spintronics, magnetic semiconductors, properties of magnetic multilayers, magnetoresistive materials and structures, magnetic oxides, and more. Novel superconducting and magnetic materials are complex compounds, and the journal publishes articles related to all aspects of their study, such as sample preparation, spectroscopy and transport properties, as well as practical applications.

Commonly used title abbreviations: JOSC

- A highly acclaimed journal offering peer-reviewed original papers, conference proceedings and review articles examining all aspects of superconductivity
- Covers spintronics, magnetic semiconductors, properties of magnetic multilayers, magnetoresistive materials and structures, magnetic oxides, and more
- Examines sample preparation, spectroscopy and transport properties, as well as practical applications
- 98% of authors who answered a survey reported that they would definitely publish or probably publish in the journal again

Editor-in-Chief

Vladimir Z Kresin

Co-Editors

V.P.S. Awana, Israel Felner, Sergei Ovchinnikov

Publishing model

Hybrid. Open Access options available

1.130 (2018) Impact factor	**25 days** Submission to first decision	**182,725 (2018)** Downloads
0.982 (2018) Five year impact factor	**54 days** Submission to Acceptance	

For authors

Submission guidelines

Ethics & disclosures

Contact the journal

Submit manuscript

Subscribe

125,21 €

Note this is only the net price. Taxes will be calculated during checkout.

Subscribe to this journal

- ✓ Immediate online access
- ✓ Full Journal access includes all articles
- ✓ Downloadable in PDF
- ✓ Subscription expires 31/12/2020

Activités Navigateur Web Firefox ▾ 8 janv. 10:20

Journal of Superconductivity and Novel Magnetism | Home - Mozilla Firefox

Journal of Superconduct X | CAS Source Index (CASS X | +

https://www.springer.com/journal/10948 67 %

Journal updates

Letters Section Edited by K.A. Müller

Nobel Laureate K.A. Müller leads a section of the journal called "Letters." These are short communications which are reviewed and published on an accelerated schedule.

View all updates ›

About this journal

Electronic ISSN	Print ISSN
1557-1947	1557-1939

Abstracted and indexed in

- Chemical Abstracts Service (CAS)
- Current Contents/Physical, Chemical and Earth Sciences
- EBSCO Academic Search
- EBSCO Applied Science & Technology Source
- EBSCO Computers & Applied Sciences Complete
- EBSCO Discovery Service
- EBSCO Energy & Power Source
- EBSCO Engineering Source
- EBSCO OmniFile
- EBSCO STM Source
- EBSCO Science Full Text Select
- EI Compendex
- Gale
- Gale Academic OneFile
- Google Scholar
- INIS Atomindex
- INSPEC
- Institute of Scientific and Technical Information of China
- Japanese Science and Technology Agency (JST)
- Journal Citation Reports/Science Edition
- Naver
- OCLC WorldCat Discovery Service
- ProQuest-ExLibris Primo
- ProQuest-ExLibris Summon
- SCImago
- SCOPUS
- Science Citation Index
- Science Citation Index Expanded (SciSearch)
- WTI Frankfurt eG

Copyright information

Rights and permissions

Springer Nature policies

Springer

Publish with us	Discover content	Other services	About Springer	Legal
Authors & Editors	SpringerLink	Instructors	About us	General term & conditions
Journal authors	Books A-Z	Librarians (Springer Nature)	Help & Support	Rights & permissions
Publishing ethics	Journals A-Z	Societies and Publishing Partners	Contact us	Privacy
Open Access & Springer	Video	Advertisers	Press releases	How we use cookies
		Shop on Springer.com	Impressum	Manage cookies
				Accessibility

SPRINGER NATURE

2- L’abstract de l’article ou toutes informations référencées par la base de données d’indexation (preuves d'indexation)

PREUVE D'INDEXATION DANS SCOPUS

Activités Navigateur Web Firefox ▾ 8 janv. 09:57

Scopus preview - Scopus - Sources - Mozilla Firefox

Scopus preview - Scopus

https://www.scopus.com/sources.uri#

Scopus Preview

Author search Sources Create account Sign in

Sources

Title | Enter title | Find sources

Title: Journal Of Superconductivity And Novel Magnetism ×

1 result

Download Scopus Source List | Learn more about Scopus Source List

All | Export to Excel | Save to source list

View metrics for year: 2018

	Source title	CiteScore	Highest percentile	Citations 2018	Documents 2015-17	% Cited	SNIP	SJR	Publisher
1	Journal of Superconductivity and Novel Magnetism	1.12	37% 246/397 Condensed Matter Physics	1 551	1 382	49	0.586	0.291	Springer Nature

^ Top of page

https://www.scopus.com/sources.uri#

Source details

Feedback › Compare sources ›

Journal of Superconductivity and Novel Magnetism

Formerly known as: Journal of Superconductivity

Scopus coverage years: from 1996 to 2019

Publisher: Springer Nature

ISSN: 1557-1939 E-ISSN: 1557-1947

Subject area: Physics and Astronomy: Condensed Matter Physics | Materials Science: Electronic, Optical and Magnetic Materials

View all documents › Set document alert Save to source list Journal Homepage

CiteScore 2018
1.12

SJR 2018
0.291

SNIP 2018
0.586

CiteScore | CiteScore rank & trend | CiteScore presets | Scopus content coverage

CiteScore 2018

Calculated using data from 30 April, 2019

1.12 = Citation Count 2018 / Documents 2015 - 2017* = 1 551 Citations › / 1 382 Documents ›

*CiteScore includes all available document types

View CiteScore methodology › CiteScore FAQ ›

CiteScoreTracker 2019

Last updated on 08 December, 2019
Updated monthly

1.34 = Citation Count 2019 / Documents 2016 - 2018 = 1 939 Citations to date › / 1 452 Documents to date ›

CiteScore rank

Category	Rank	Percentile
Physics and Astronomy — Condensed Matter Physics	#246/397	37th
Materials Science — Electronic, Optical and Magnetic Materials	#142/225	36th

View CiteScore trends › Add CiteScore to your site

Metrics displaying this icon are compiled according to Snowball Metrics, a collaboration between industry and academia.

PREUVE D'INDEXATION DANS
WEB OF SCIENCE

Activités Navigateur Web Firefox 8 janv. 10:27

Web of Science Master Journal List - Journal Profile - Mozilla Firefox

CAS Source Index (CASSI X | Web of Science Master J X

https://mjl.clarivate.com/journal-profile

Web of Science Group

Search Journals | Match Manuscript | Downloads | Scope Notes | Help Center

Welcome, YESSOUFOU Rachidi

Settings | Log Out

General Information

Web of Science Coverage

Journal Metrics

Peer Review Information

Return to Search Resul

JOURNAL OF SUPERCONDUCTIVITY AND NOVEL MAGNETISM

ISSN / eISSN **1557-1939 / 1557-1947**

Publisher **SPRINGER, 233 SPRING ST, NEW YORK, USA, NY, 10013**

General Information

Journal Website	Visit Site	**Publisher Website**	Visit Site
1st Year Published	2006	**Frequency**	Monthly
Issues Per Year	12	**Country / Region**	UNITED STATES OF AMERICA
Primary Language	English	**Submission Website**	Visit Site

Some general information was sourced from the Directory of Open Access Journals and/or Transpose.

Web of Science Master Journal List - Journal Profile - Mozilla Firefox

https://mjl.clarivate.com/journal-profile

Web of Science Coverage

Scope Notes

Web of Science Core Collection

Science Citation Index Expanded (SCIE)

Additional _Web of Science_ Indexes

Current Contents Physical, Chemical & Earth Sciences

Essential Science Indicators

Categories: Physics, Applied | Physics, Condensed Matter | Physics | Applied Physics/Condensed Matter/Materials Science

Log into *Web of Science* to discover research literature from this journal.

Journal Metrics

2018 Journal Impact Factor 1.130

3- Tiré-à-part de l'article

Mean-Field and Monte Carlo Studies of the Magnetic Properties of a Spin-7/2 and Spin-5/2 Ising Bilayer Film

M. Karimou, R. A. Yessoufou, G. D. Ngantso, F. Hontinfinde & A. Benyoussef

Journal of Superconductivity and Novel Magnetism

ISSN 1557-1939
Volume 32
Number 6

J Supercond Nov Magn (2019)
32:1769-1779
DOI 10.1007/s10948-018-4876-4

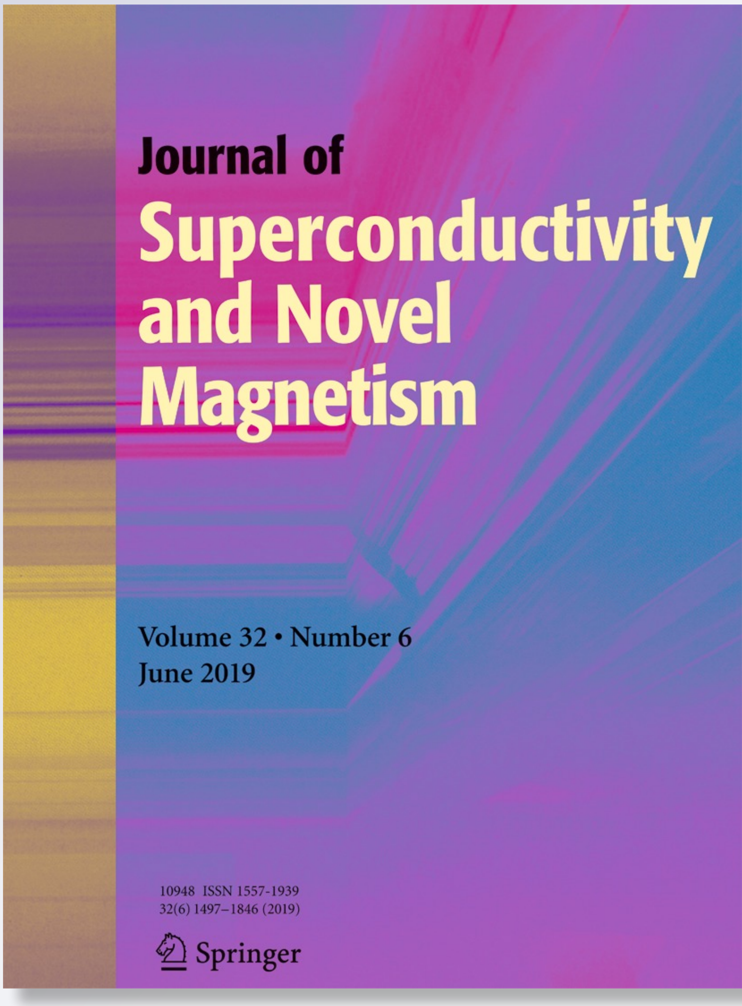

Springer

Journal of Superconductivity and Novel Magnetism (2019) 32:1769–1779
https://doi.org/10.1007/s10948-018-4876-4

ORIGINAL PAPER

Mean-Field and Monte Carlo Studies of the Magnetic Properties of a Spin-7/2 and Spin-5/2 Ising Bilayer Film

M. Karimou[1] · R. A. Yessoufou[1,2] · G. D. Ngantso[3,4] · F. Hontinfinde[1,2] · A. Benyoussef[3,5]

Received: 6 July 2018 / Accepted: 10 September 2018 / Published online: 18 September 2018

Abstract

We use standard Monte Carlo simulations based on the Metropolis algorithm and mean-field calculations to investigate the magnetic properties of an Ising bilayer film consisting of two superposed ferromagnetic squared lattices A and B whose magnetic atoms have spin 7/2 and 5/2 respectively. Crystal-field and external magnetic field effects on the spins are considered in the model. The magnetic order parameters and response functions are calculated as functions of the temperature for selected values of the model parameters and this enables one to devise thermal phase diagrams by both methods. Our calculations only reveal second-order phase boundaries. Under appropriate conditions, compensation point phenomena are detected in the calculations below the critical temperatures. When the system is exposed to the external magnetic constraint, attracting hysteresis phenomena are sometimes generated. The temperature dependence of the coercitive field for various values of the crystal-field is singled out.

Keywords Monte Carlo simulations · Mean-field calculations · Ising bilayer film · Compensation temperature · Temperature phase diagram · Hysteresis phenomena

1 Introduction

The theoretical investigation of magnetic systems formed by sublattices of alternately unequal opposite magnetic moments has generated valuable results and an increasing interest among condensed matter physicists [1, 2]. Besides the fundamental aspects, recent developments on the subject have shown real advances in the synthesis of novel magnets for potential technological uses: thermomagnetic data storage and retrieval, magneto-optical recording devices, etc [3–5]. Theoretical and numerical tools of statistical mechanics often used in the studies are mean-field (MF) theory [6, 7], effective-field theory (EFT) [8–10], exact recursion relations (ERR) [11], Monte Carlo (MC) simulations [12, 13], etc. Some recent interesting works in the field could be mentioned. Kaneyoshi [14] and Kaneyoshi et al. [15] examined the effect of transverse fields on a mixed-spin (1/2 and 1) Ising bilayer film in some interesting theoretical developments. The aims were to explain the negative magnetization that appears in some molecular-based ferrimagnets. Generated results bear resemblance with behaviors observed in some crystalline ferrimagnetic alloys. Kaneyoshi et al. [16, 17] also studied a bipartite ferrimagnets like $MnCu(pba-OH)(H_2)_3$ on the basis of the EFT with spin correlations first introduced by Honnura and Kaneyoshi [18]. Very recently, Bahlagui et al. [19, 20] addressed by means of MC simulations a mixed-spin (7/2, 5/2) Ising ferrimagnetic system on a square lattice which could describe magnetic properties of the $GdFeO_3$ as demonstrated by the application of Hund's rule to the Gd and Fe ions. In the previous studies, the influence of the strength of the single-ion anisotropy interaction on the magnetic properties, in particular, on the compensation temperature has been thoroughly discussed. The existence of compensation phenomenon in a magnetic system due to a complete cancellation of sublattice magnetizations

✉ R. A. Yessoufou
yesradca@yahoo.fr

1 Institute of Mathematics and Physical Sciences (IMSP), Porto-Novo, Benin

2 Department of Physics, University of Abomey-Calavi, Cotonou, Benin

3 LMPHE, Faculty of Sciences, Mohammed V University, Rabat, Morocco

4 GSMC, Faculty of Sciences and Techniques, Marien Ngouabi University, Brazzaville, Congo

5 Hassan II Academy of Sciences and Technology, Rabat, Morocco

below the critical temperature T_c, has been pointed out in several works [12, 13, 19, 20] and has obvious technological significance. Indeed, a small amount of driving field is required to achieve in this system, magnetic pole reversal or the sign change of the total magnetization [21–23]. On the other hand, spin Ising models have been also considered to examine very small systems, such as nanoparticles with core-shell structure [24–26]. It is worthwhile to mention that the latters are also receiving considerable attention these last twenty years because of their possible applications in permanent magnets, microwave absorption [27, 28], etc.

In this paper, a spin-7/2 and spin-5/2 Ising model is introduced through a squared bilayer system and studied by MF and MC calculations. It should be noted that such system is very useful to simulate thin magnetic films that consist of various layered structures or superlattices. Insulating ferromagnets built up from several magnetic sublattices are typical examples in the field (see ref. [8] and references therein). Here, the thermal behaviors of the total and layer magnetizations of the film are calculated by both methods. We are interested in the influence of the single-ion anisotropy (crystal-field) interaction and the external magnetic constraint on the magnetic properties of the system. In this context, several finite-temperature phase diagrams have been plotted in the model parameters' space. Of particular importance is the dependence of the hysteresis phenomenon that emerged on model parameters when the external field is applied. Numerical results derived by both methods are often compared and agreement between them looks impressive.

The outline of the paper is as follows. In Section 2, the model Hamiltonian is specified and the MF equations of state are derived. Section 3 gives the MC simulations procedure. In Section 4, our obtained results are presented and discussed. Finally, a brief conclusion is presented in Section 5.

2 Formulation of the Model and Its Mean-Field Solution

The bilayer Ising film model consists of spin particles interacting with an external magnetic field. Two square lattices with spins $S = 7/2$ and $\sigma = 5/2$ are considere (Fig. 1). We refer to these layers as layer A and B respectively. The Hamiltonian of the model is written as follows:

$$H = -J_1 \sum_{\langle i,j\rangle} S_i S_j - J_2 \sum_{\langle m,n\rangle} \sigma_m \sigma_n - J_3 \sum_{\langle i,m\rangle} S_i \sigma_m - D_1 \sum_i (S_i)^2 - D_2 \sum_m (\sigma_m)^2 - h \sum_i S_i - h \sum_m \sigma_m \quad (1)$$

where J_1 and J_2 are intralayer exchange coupling constants for the first and second layers, respectively, and J_3 is the interlayer coupling constant over adjacent neighboring sites of layers. D_1 and D_2 are the crystal-fields acting on spins of layers A and B respectively. h is the external magnetic field.

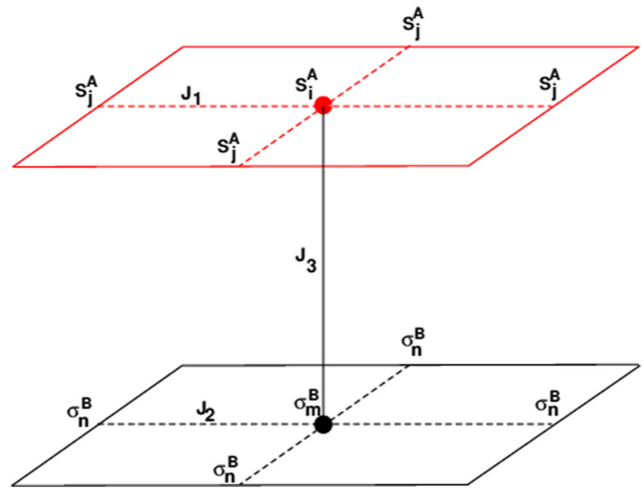

Fig. 1 Schematic representation of the bilayer magnetic film. Layer A and layer B refer to the upper and lower layers containing spins labeled S_i^A, S_j^A and σ_m^B, σ_n^B

The approximated free energy of this system is obtained from a variational method based on the Bogoliubov inequality,

$$F(H) \leq \Phi \equiv F_0(H) + \langle H - H_0\rangle_0, \quad (2)$$

where $F(H)$ is the true free energy of the model described by the Hamiltonian given in (1). $F_0(H)$ is the average free energy of a trial Hamiltonian H_0 which depends on variational parameters. $\langle H - H_0\rangle_0$ denotes a thermal average of the value $H - H_0$ over the ensemble defined by the trial Hamiltonian H_0.

In this work, we use one of the simplest choices for this trial Hamiltonian given by:

$$H_0 = -\sum_i (\alpha_S S_i + D_1 S_i^2) - \sum_m (\alpha_\sigma \sigma_m + D_2 \sigma_m^2), \quad (3)$$

where α_S and α_σ are two variational parameters related to the molecular field acting on the two layers A and B respectively.

By evaluating (2), the expression of the free energy per site by MF reads:

$$\begin{aligned}\Phi = & -\frac{1}{\beta}\left(\ln\left[2e^{\frac{49\beta D_1}{4}}\cosh(\frac{7}{2}\beta\alpha_S) + 2e^{\frac{25\beta D_1}{4}}\cosh\left(\frac{5}{2}\beta\alpha_S\right)\right.\right.\\ & \left.\left. + 2e^{\frac{9\beta D_1}{4}}\cosh\left(\frac{3}{2}\beta\alpha_S\right) + 2e^{\frac{\beta D_1}{4}}\cosh\left(\frac{1}{2}\beta\alpha_S\right)\right]\right)\\ & -\frac{1}{\beta}\left(\ln\left[2e^{\frac{25\beta D_2}{4}}\cosh\left(\frac{5}{2}\beta\alpha_\sigma\right) + 2e^{\frac{9\beta D_2}{4}}\cosh\left(\frac{3}{2}\beta\alpha_\sigma\right)\right.\right.\\ & \left.\left. + 2e^{\frac{\beta D_2}{4}}\cosh\left(\frac{1}{2}\beta\alpha_\sigma\right)\right]\right) - J_1 q_1 m_A^2 + \alpha_S m_A - J_2 q_2 m_B^2\\ & + \alpha_\sigma m_B - J_3 q_3 m_A m_B - h m_A - h m_B. \end{aligned} \quad (4)$$

To get the expressions of the order parameters describing the magnetizations m_A and m_B, one should minimize the free energy. By partially deriving (4) with respect to α_S and α_σ, one gets:

$$\alpha_S = J_1 m_A q_1 + J_3 m_B q_3 + h,$$
$$\alpha_\sigma = J_2 m_B q_2 + J_3 m_A q_3 + h,$$

where q_1, q_2, and q_3 are respectively numbers of neighbor's interactions in sublattice A, sublattice B and between sublattices A and B for a given spin of the system. The calculations lead to the following state equations:

$$m_A = \frac{7\sinh\left(\frac{7}{2}\beta\alpha_S\right) + 5e^{(-6\beta D_1)}\sinh\left(\frac{5}{2}\beta\alpha_S\right) + 3e^{(-10\beta D_1)}\sinh\left(\frac{3}{2}\beta\alpha_S\right) + e^{(-12\beta D_1)}\sinh\left(\frac{1}{2}\beta\alpha_S\right)}{2\cosh\left(\frac{7}{2}\beta\alpha_S\right) + 2e^{(-6\beta D_1)}\cosh\left(\frac{5}{2}\beta\alpha_S\right) + 2e^{(-10\beta D_1)}\cosh\left(\frac{3}{2}\beta\alpha_S\right) + 2e^{(-12\beta D_1)}\cosh\left(\frac{1}{2}\beta\alpha_S\right)}.$$

$$m_B = \frac{5\sinh\left(\frac{5}{2}\beta\alpha_\sigma\right) + 3e^{(-4\beta D_2)}\sinh\left(\frac{3}{2}\beta\alpha_\sigma\right) + e^{(-6\beta D_2)}\sinh\left(\frac{1}{2}\beta\alpha_\sigma\right)}{2\cosh\left(\frac{5}{2}\beta\alpha_\sigma\right) + 2e^{(-4\beta D_2)}\cosh\left(\frac{3}{2}\beta\alpha_\sigma\right) + 2e^{(-6\beta D_2)}\cosh\left(\frac{1}{2}\beta\alpha_\sigma\right)}.$$

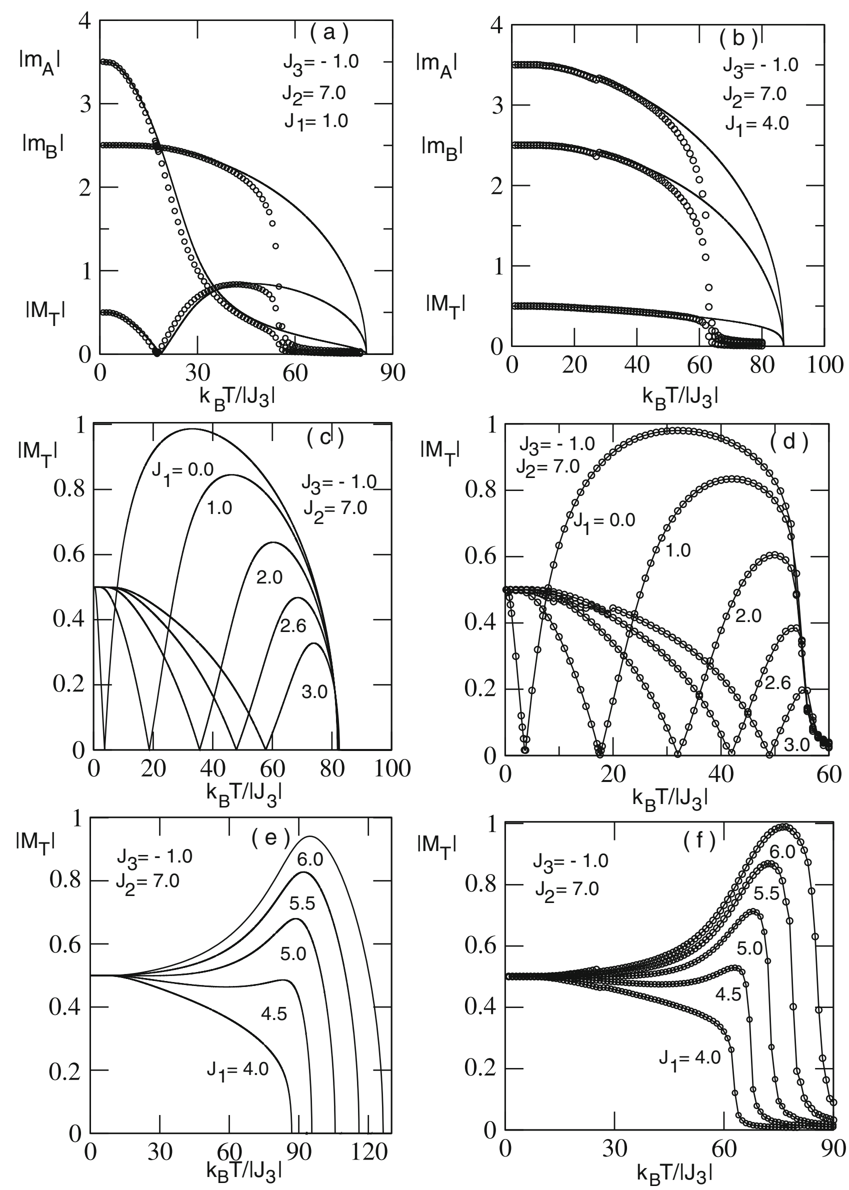

Fig. 2 Variations of the total magnetization $|M_T|$ and the sublattice magnetizations $|m_A|$, $|m_B|$ as functions of the temperature for $J_3 = -1.0$, $J_2 = 7$ and for selected values of the coupling constant J_1 (panels **a** and **b**) by both methods. Thermal variations of the the total magnetization $|M_T|$ when the values of J_1 is varied for fixed values of J_3 and J_2 written in the panels (panel **c** to panel **f**). Here, right panels contain MC results while left ones are for MF results

In order to determine the compensation temperature, one has to define the global magnetization M_T of the model which is given by:

$$M_T = \frac{m_A + m_B}{2}. \tag{5}$$

To study the model in detail and single out the influence of the applied magnetic field on the magnetic properties of the model, one has to examine the thermal variations of the order parameters and the response functions e.g., the magnetic susceptibilities defined as follows:

$$\chi_T = \chi_A + \chi_B = \left(\frac{\partial m_A}{\partial h}\right)_{h=0} + \left(\frac{\partial m_B}{\partial h}\right)_{h=0} \tag{6}$$

3 The Monte Carlo Simulation Method

The sample consists of two superposed squared lattices A and B (Fig. 1). The upper lattice (A) sites are occupied by spins $\sigma = 7/2$ and the lower (B) by spins $S = 5/2$. Typically, each lattice of the sample contains $N = L \times L = 10^4$ sites. Periodic boundary conditions are imposed on the layers and the standard Metropolis algorithm [19, 20, 29] is adopted for the simulations. The latters are propagated as follows. A site is randomly selected in the system and the flip of its spin is attempted. For that, a spin value is randomly selected within the possible projections with a uniform distribution. The probability of each configuration is proportional to the Boltzmann factor and another random number is chosen to decide or reject the attempted move. Physical quantities of interest are calculated after $N_S = 10^5$ Monte Carlo steps per site are performed. The first $N_E = 10^4$ steps are considered for thermal equilibration and then discarded from the averaging procedure. The lattice magnetizations are calculated as follows:

$$m_A = \frac{1}{N}\sum_{i=1}^{N} S_i \tag{7}$$

$$m_B = \frac{1}{N}\sum_{i=1}^{N} \sigma_i \tag{8}$$

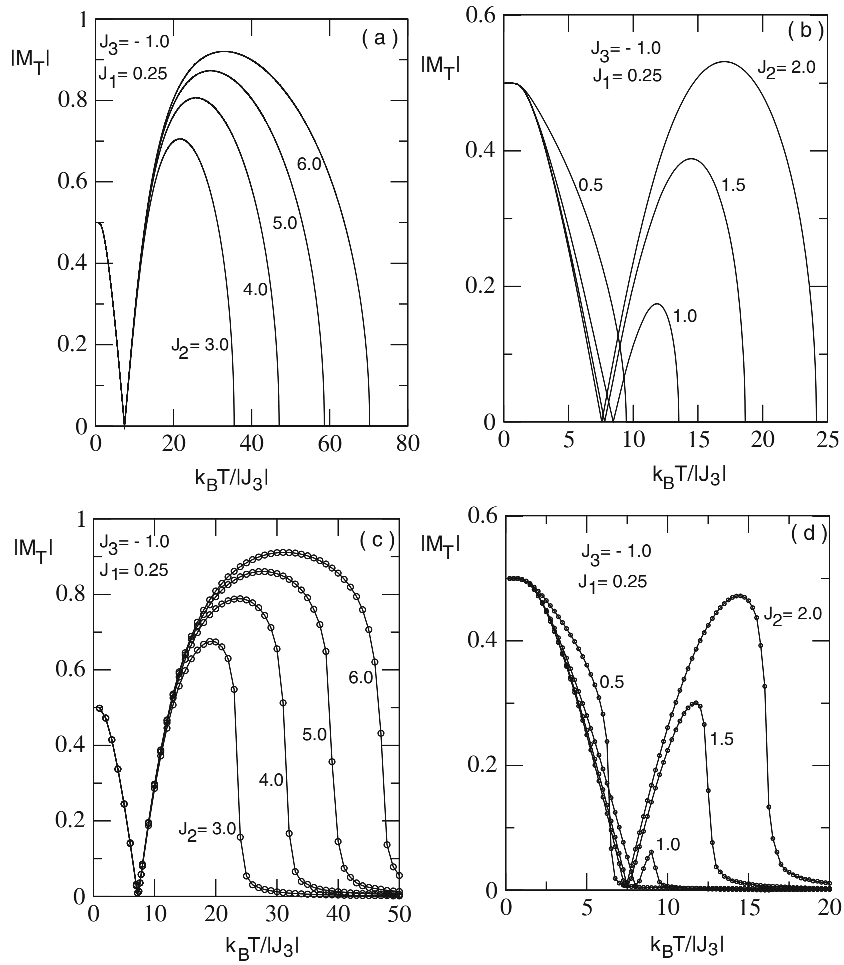

Fig. 3 Variations of the total magnetization $|M_T|$ as a function of the temperature for $J_3 = -1.0$, $J_1 = 0.25$ and for selected values of J_2. Panels a and b contains MF results while panels c and d are for MC results

The total magnetization M_T is given by the average value:

$$M_T = (m_A + m_B)/2 \quad (9)$$

The critical temperature T_c is defined by $M_T(T_c) = m_A(T_c) = m_B(T_c) = 0$ when the temperature is increased from $T = 0$. The magnetic susceptibility is calculated by the formula:

$$\chi_T = << (\overline{\sigma} + \overline{S})^2 > - M_T^2 >, \quad (10)$$

where $\overline{\sigma}$ and $\overline{S}$ are the averaged layer magnetizations at a given step of the simulation and $< . >$ denotes a statistical average over the $(N_S - N_E)$ MC steps needed to reach the steady state, starting from thermal equilibrium.

4 Results and Discussions

We first look for the effects of the coupling constant J_1 on the system magnetizations, setting $J_2 = 7$ and $J_3 = -1$. Only ferromagnetic inlayer J_1 interaction values are used to compute m_A, m_B and M_T. This enables us to first check the accuracy of our numerical results by MF and MC when the temperature is varied. In Fig. 2a, $J_1 = 1.0$ whereas in Fig. 2b, $J_1 = 4.0$. In both panels, it could be noted that the layer magnetizations have their saturation values $|m_A| = 3.5$ and $|m_B| = 2.5$ at $T = 0$ and when the temperature T is varied, they fall from these values, then decrease monotonically and finally vanish almost at the same temperature when MF or MC computations are separately considered. On the contrary, it should be noted that in the panel a, M_T vanishes at the crossing point of

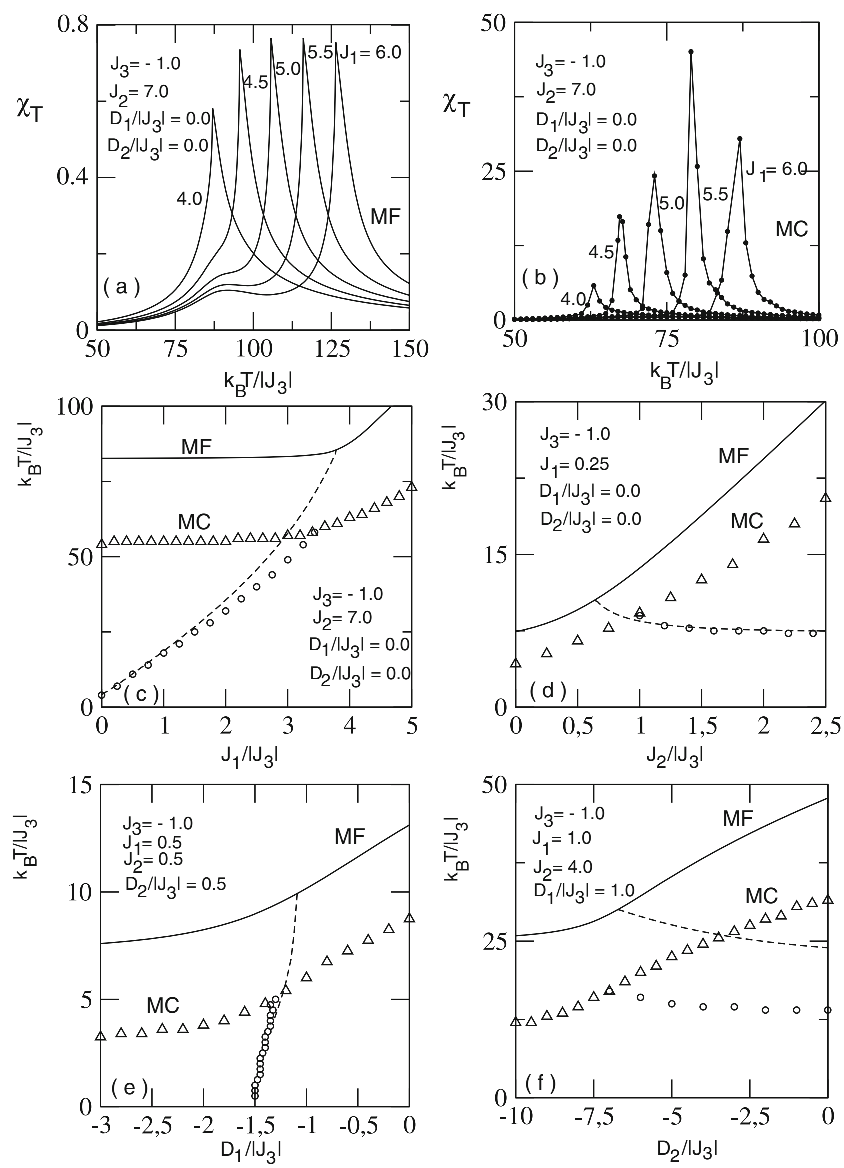

Fig. 4 Total magnetic susceptibility curves χ_T of the magnetic film by mean-field theory and Monte Carlo simulations for selected values of J_1 when $J_3 = -1$, $J_2 = 7$ and $D_1/|J_3| = D_2/|J_3| = 0.0$ (panels **a** and **b**). Temperature phase diagrams by MF and MC in different planes for selected values of the model parameters (panels **c** to **f**). Full lines are critical lines and dashed lines are compensation lines, all found by MF calculations whereas open triangles/circles denote critical/compensation points obtained by MC simulations

$m_A(T)$ and $m_B(T)$ well before T_c. This particular point is known as the compensation temperature that is noted T_{comp}. At T_{comp}, both layers have opposite magnetic moments giving rise to zero global film magnetic moment. The values of T_{comp} by MF and MC are almost the same. This reveals that T_{comp} could be determined with more accuracy than T_c through the present investigation. In panel b, the compensation phenomenon is absent since m_A and m_B do not cross each other and m_A, m_B and M_T all vanish at the same temperature T_c. First, let us notice that the value of T_c obtained by MF and MC are different, $T_c(MC) < T_c(MF)$. Indeed, values of critical temperatures calculated by both methods are $kT_c/|J_3| \simeq 82$ for MF calculations whereas for MC calculations $kT_c/|J_3| \simeq 55$ for $J_1 = 1$. But for $J_1 = 4$, $kT_c/|J_3| \simeq 87$ for MF calculations whereas $kT_c/|J_3| \simeq 63$ for MC simulations. This discrepancy originates from the fact that the MF calculations, neglect correlations in spin fluctuations whereas they are important in the neighborhood of T_c. The existence of T_{comp} in ferrimagnets is of technological importance and enhances most physicists' interest in the field. Far from that region, ie in the relatively low temperature range, the agreement between both results by MF and MC appears evident and suggests that either MF or MC procedure could be adopted in order to get reliable values of the magnetizations. The influence of model parameters on T_{comp} has been intensively studied in several previous works [12, 19, 21], especially the case of single-ion anisotropy. In panels c,d,e,f of Fig. 2, the influence of the coupling constant J_1 was studied when the two layers interact antiferromagnetically. Figure 2c, d indicates a good qualitative agreement between MF and MC results and suggest that for $J_1 \leq 3$, T_{comp} exists and increases with increasing values of the coupling constant J_1. The influence of intralayer coupling constants as J_1 on the compensation temperature is then very important. On the contrary, the value of T_c through both panels is not affected when the coupling constant J_1 is varied, neither by MC nor by MF computations, at least in the values of J_1

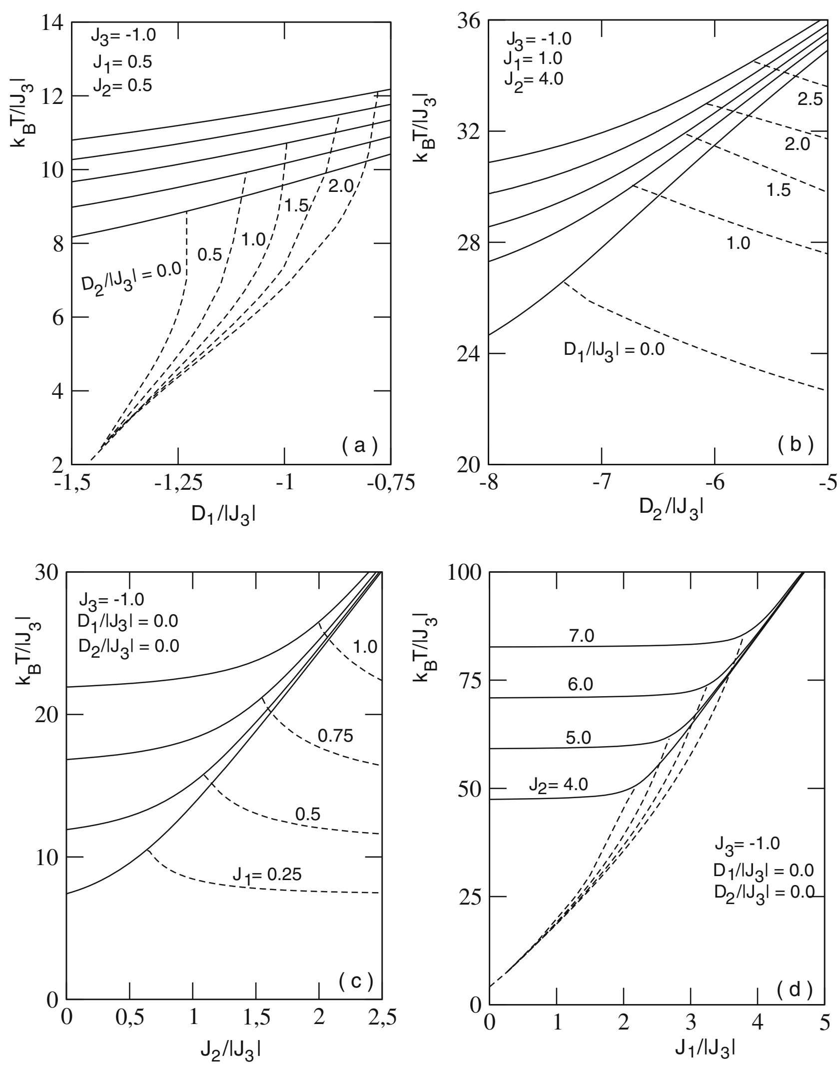

Fig. 5 Phase diagrams of the system illustrated in the $(D_1/|J_3|, k_BT/|J_3|)$, $(D_2/|J_3|, k_BT/|J_3|)$, $(J_2/|J_3|, k_BT/|J_3|)$ and $(J_1/|J_3|, k_BT/|J_3|)$ planes by mean-field calculations, full/dashed lines are critical/compensation lines

range selected. The situation above this range is presented in Fig. 2e, f. Evidently, we also get good agreement between results by MC and MF which showed the absence of T_{comp} for $J_1 \geq 4$. The results reported here about Fig. 2 are quite similar to those displayed in Fig. 4 of Ref. [20] although their model and the one studied here are different. Here, a bilayer is considered whereas in their work, a single layer with two sublattices of unequal magnetic moments has been investigated. It is worthwhile to mention that saturated values of M_T got at $T = 0$ indicate that for the selected values of the model parameters, the ground state configuration is $(-7/2, +5/2)$. This phase does not change up to T_c which is the onset of the disordered paramagnetic phase. As shown in ref. [19], the behavior of $T_c - T_{comp}$ or simply T_{comp} could be studied as a function of values of model parameters, e.g., the coupling constant J_1.

Other interesting features of the model are revealed in Fig. 3 at fixed values of J_1 and J_3 and varying values of J_2. In the panel a, one gets a fixed T_{comp} which is associated to several values of T_c when $J_2 \geq 3$. The T_{comp} does not exist for $J_2 \leq 0.5$. Between these two limiting values, T_{comp} varied with J_2. Let us remark that after the maximum, the total magnetization (M_T) curves look parallel in each panel when MF and MC calculations are considered. This means that T_c changes almost linearly with J_2 at least for $J_2 \geq 1.0$.

In order to precisely locate T_c when values of model parameters are varied, the film magnetic susceptibility is calculated by MF and MC and some of the results have been checked by the specific heat computation by MC simulations. The numerical results for some selected values of the model parameters are displayed in Fig. 4a, b. The susceptibility curves show peaks whereas the order

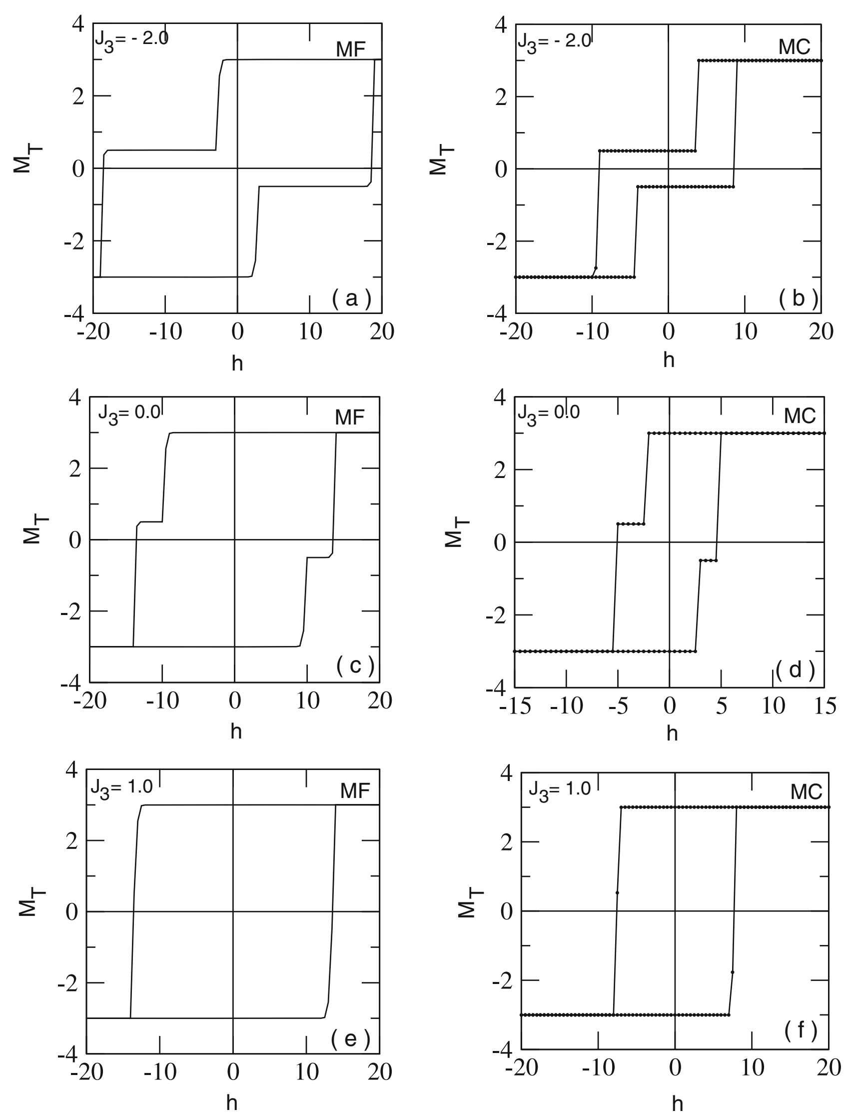

Fig. 6 The effect of the coupling constant J_3 on hysteresis loop patterns of the magnetic film for $J_1 = J_2 = 1.0$, $T = 1.0$ and $D_1/|J_3| = D_2/|J_3| = 1.0$. Left panels contain MF results and the right ones, those calculated by MC simulations

parameters vanish continuously. These are true features of the existence of second-order phase transitions. Using values of these critical temperatures detected in this way, some finite-temperature phase diagrams are plotted in the remaining panels of Fig. 4. Phase boundaries are exclusively of second order and appear almost parallel when MF and MC procedures are compared. On the contrary, T_{comp} curves coincide in a wide range of the varying model parameter. Different observations noted in Fig. 3 are revealed in Fig. 4d. There, we note that for large values of the coupling constant J_2, the compensation curves become parallel to the $J_2/|J_3|$-axis with a constant value of T_c. As previously stated, the T_c-line in this panel is almost linear for $J_2 \geq 1$. Below the critical lines, magnetic ordered film is expected. Above, the disordered paramagnetic phase prevails. Since critical lines generated by MF and MC are almost parallel, other phase boundaries are presented in Fig. 5 only by MF.

The latters extend MF results displayed in Fig. 4. A direct analysis of the phase boundaries suggest that for sufficiently negative values of coupling constants, phase boundaries are parallel in most cases. Above the critical lines, paramagnetic phases should prevail.

From now on, let us discuss the last interesting results. It is well-known that the emergence of hysteresis phenomenon is a suitable tool to describe the reaction of a multi-agent system when subjected to external perturbations. It has been observed in several metallic ferromagnets [30, 31] and describes the delay of magnetization or generally that of the effect on the cause. It could be observed in the nature in different contexts (see [31–33] and references therein) and used for example in high frequency device applications (see [34]). Essaoudi et al. [35] addressed sometimes ago, by means of EFT within a probability distribution technique [36] a mixed-spin (1/2, 3/2) bilayer

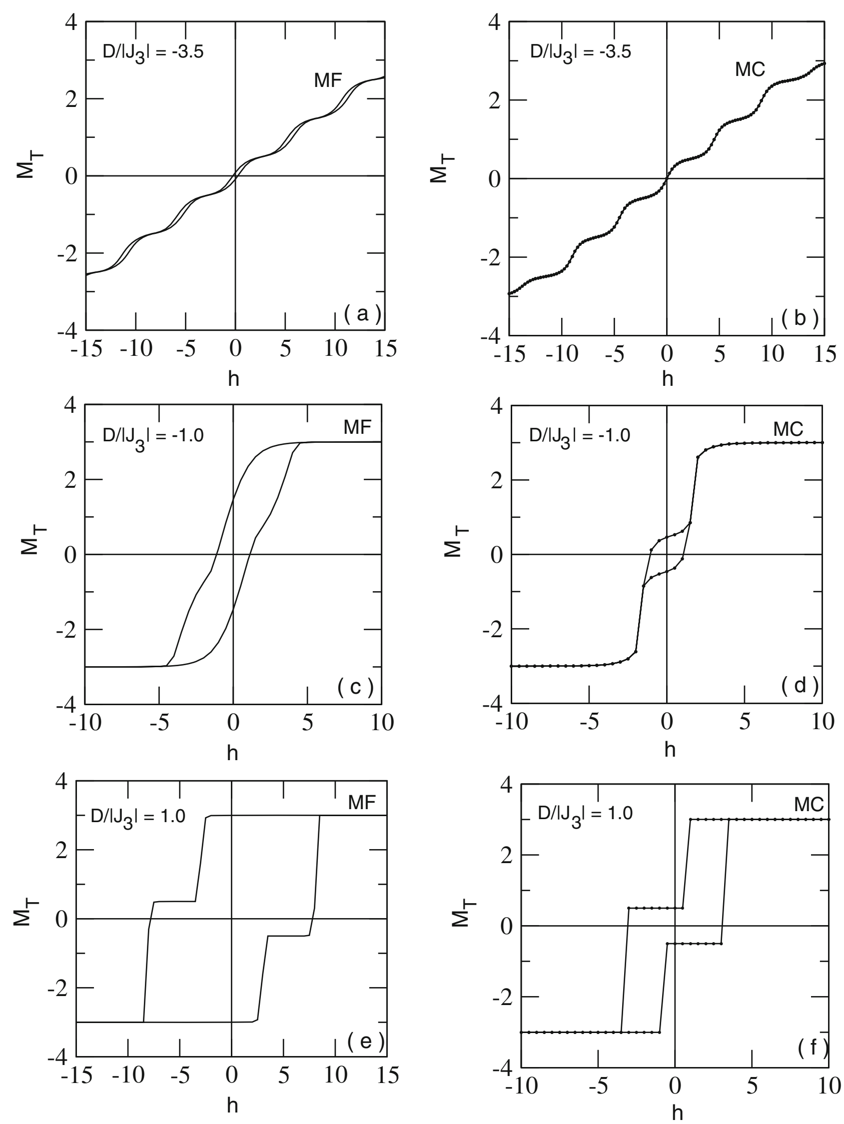

Fig. 7 The effect of the crystal-field strength D on hysteresis loops for $J_1 = J_2 = 0.5$, $T = 1.0$ and $J_3 = -0.5$ when the external field is set on the system. Left panels contain MF results and the right ones, those found by MC simulations

Ising model and reported such phenomenon. Here, it is revealed when the external magnetic field is set on the system. In view to study the behavior of the hysteresis phenomenon with the interlayer coupling constant J_3, the following values of the model parameters are retained: $J_1 = 0.5$, $J_2 = 0.5$, $D_1/|J_3| = D_2/|J_3| = D/|J_3| = 1.0$, $T = 1.0$. In Fig. 6, results by MF (left panels) and MC (right panels) are presented when the interlayer coupling constant J_3 is increased from negative values. Qualitative agreement between the MF and MC results is evident. The loop pattern starts with a large double loop and as J_3 increases, the deformation disappears leading to a single central loop. Such double hysteresis loop pattern has been observed in ferroelectric superlattices [30] and may be typical of antiferro-structure of dipoles or magnetic moments when coupled layers have the same thickness as in the present case. One can conclude that in Fig. 6a, the behavior of the system under study is then antiferromagnetic. The interesting fact is that with $J_3 = 0$, the system is still then globally antiferromagnetic for the selected values of the model parameters since the double hysteresis loop is still present. In all three panels, the remanent magnetization coincides with the saturation value of the film total magnetization. In Fig. 7, the crystal-field strength effect is examined. We used: $J_1 = 0.5$, $J_2 = 0.5$, $J_3 = -0.5$ and $T = 1.0$. For sufficiently negative values of $D/|J_3|$, loops are almost absent and one gets multistep behavior of the film magnetization, even after the field reversal. Double loop appears with increasing values of the parameter D. There exists some few differences in the loop forms obtained there by MF and MC results. In Fig. 8, the qualitative agreement between the forms of the loops is observed when the temperature-dependence of the loop pattern is evaluated. Here, we retained: $J_1 = 0.5$,

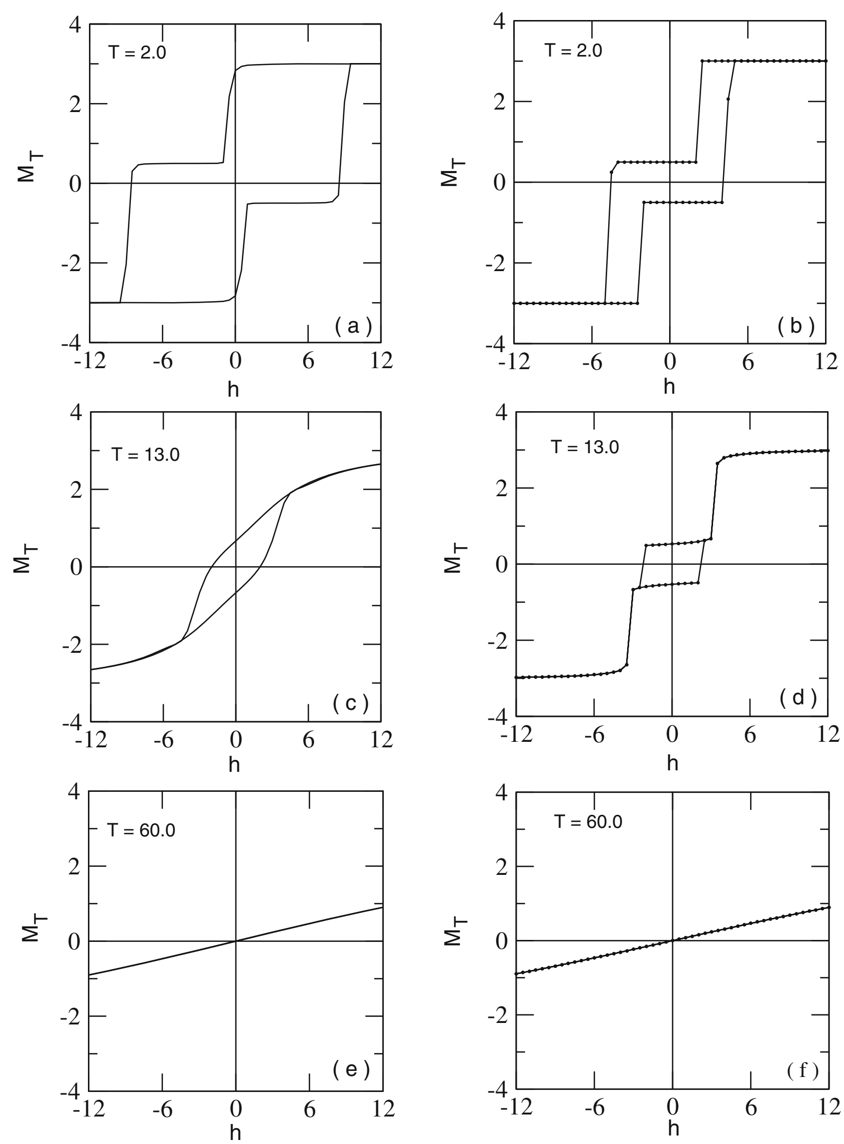

Fig. 8 The temperature-dependence of hysteresis loop patterns for $J_1 = J_2 = 0.5$, $J_3 = -1.0$ and $D_1/|J_3| = D_2/|J_3| = 1.0$. Left panels contain MF results and the right ones, those computed by MC simulations

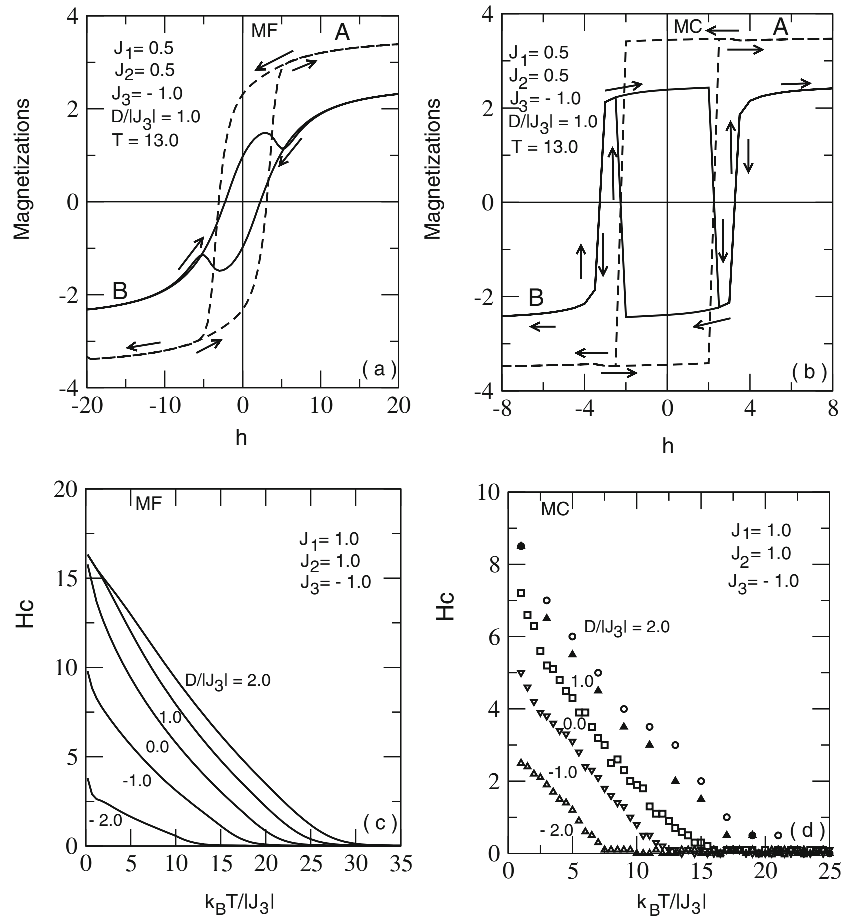

Fig. 9 Sublattice hysteresis loops corresponding to Fig. 8 by MF (panel **a**) and MC (panel **b**). In panels **c** and **d**, the temperature-dependence of the coercitive field is shown for different values of the crystal-field strength. At fixed value of this strength, the coercitive field of the magnetic film is a decreasing function of the temperature at least in the temperature range investigated

$J_2 = 0.5$, $D_1/|J_3| = D_2/|J_3| = D/|J_3| = 1.0$ $J_3 = -1.0$. It appears obvious that when the temperature is varied, the whole magnetic behavior of the film changes from antiferromagnetic (panels a, b) to ferromagnetic (panels c, d) and later to an almost straight line (panels e, f). The latter indicated that both layers are magnetically disordered and the hysteresis phenomenon cannot exist any more. Of particular importance is the hysteresis behavior of each layer separately. This is shown in Fig. 9a, b for results about Fig. 8c, d. As indicated by arrows in each panel, MF and MC results are qualitatively the same. For the layer A, the loop is described in the common or regular sens whereas for layer B, the inverse holds. This finally strongly decreases the area of the resulting hysteresis ferromagnetic loop.

We also study the behavior of the coercitive field as functions of the crystal-field when the temperature is raised. As it could be observed from panels c and d, results by MC and MF show very good agreement: H_c is a decreasing function of the temperature. This is partly consistent with results reported in Fig. 4 of ref. [37] where an increase is again detected after a critical value of the temperature. Fe nanoparticles show similar trends concerning the temperature dependence of the coercitive field with the temperature [38].

5 Conclusion

We used Monte Carlo simulations and mean-field theory to study a bilayer magnetic film with an Ising-type Hamiltonian. An interlayer antiferromagnetic coupling is assumed and the effect of the crystal-field or single-ion interaction is considered in the system. Our calculations generated some interesting results. First, strong qualitative agreement is observed about results generated by both methods. Second, under appropriate values of the model parameters, compensation temperatures where the global magnetization vanishes are detected. This temperature is found to be sensitive to the change of the values of the model parameters in most cases. Third, critical temperatures are obtained by the computation of the film magnetic susceptibility. This enabled us to construct the finite-temperature phase diagrams in several planes of the model parameters'space. Phase boundaries are essentially of second-order kind. Fourth, when an external magnetic field is applied, hysteresis phenomenon appeared. Under appropriate conditions, double loops are obtained indicating the antiferromagnetic behavior of the film. When values of the model parameters are varied, the nature of the loop changes and thus the thermodynamic stable phases in which the film lays on: antiferromagnetic, ferromagnetic, or paramagnetic phase. Due to the importance of the emergence of the hysteresis phenomenon, we investigate the behavior of the coercitive field with the single-ion anisotropy and the temperature. We found that this field decreases with the temperature in agreement with what is observed in some iron (Fe) nanoparticles and alloys [38] and increases with the strength of the single-ion anisotropy. In Figs. 2 and 4 of refs. [37, 39] where dynamic magnetic hysteresis properties have been studied, an increase is again observed after some critical temperature. An interesting problem is the behavior of the compensation temperature, the coercitive field and the remanent magnetizations of superlattices with several antiferromagnetic interfacial couplings. Work on the subject is in progress.

References

1. Svendsen, H., Overgaard, L., Chevalier, J., et al.: Chemistry **16**, 7215 (2010)
2. Özkan, A.: Phas. Trans. **89**, 94 (2015)
3. Mollah, T., Thiebaut, S., Verdagner, M., Veillet, P.: Science **262**, 1551 (1993)
4. Manriquez, J., Lee, G.T., Scott, R., et al.: Science **252**, 1415 (1991)
5. Jiang, W., Wei, G.Z., Zhang, Z.Z.: Phys. Rev. B **68**, 134432 (2003)
6. Kaneyoshi, T., Chen, J.C., Magn, J.: Magn. Mater. **98**, 201 (1991)
7. Wang, C.L., Xin, Y., Wang, X.S., Zhong, W.L., Zhang, P.L.: Phys. Lett. A **268**, 117 (2000)
8. Deviren, B., Canko, O., Keskin, M.: J. Magn. Magn. Mater. **320**, 2291 (2008)
9. Bouziane, T., Belaaraj, A.: Phys. Stat. Sol. (b) **214**, 387 (1999)
10. Albayrak, E.: Phys. Stat. Sol. (b) **244**, 759 (2007)
11. Karimou, M., Yessoufou, R.A., Guedje, F.K., Aïnamon, C., Hontinfinde, F.: Phas. Trans. https://doi.org/10.1080/01411594.2016.1179739 (2016)
12. Wang, W., Lv, D., Zhang, F., Bi, J., Chen, J.: J. Magn,. Magn. Mater. **385**, 16 (2015)
13. Jabar, A., Tahiri, N., Bahmad, L., Benyoussef, A.: Phys. A **462**, 1067 (2016)
14. Kaneyoshi, T.: Nanomaterials **7**(9), 256 (2017). https://doi.org/10.3390/nano7090256
15. Kaneyoshi, T., Samento, E.F., Fittipaldi, I.P.: Jpn. J. Appl. Phys. **27**, L690 (1988)
16. Kaneyoshi, T., Nakamura, Y.: J. Phys. Condens. Matter **10**, 3003 (1998)
17. Kaneyoshi, T., Nakamura, Y., Shin, S.: J. Phys: Condens. Mat. **10**, 7025 (1998)
18. Honnura, R., Kaneyoshi, T.: J. Phys. C: Sol. Stat. Phys. **12**, 3979 (1979)
19. Bahlagui, T., El Kenz, A., Benyoussef, A.: Journal of Superconductivity and Novel Magnetism, https://doi.org/10.1007/s10948-018-4698-4
20. Bahlagui, T., Bouda, H., El Kenz, A., Bahmad, L., Benyoussef, A.: Superlattices and Microstructures. https://doi.org/10.1016/j.spmi.2017.09.001 (2017)
21. Cornel, G.A., Allen, R., Mansuripur, M.: J. Appl. Phys. **53**, 77539 (1982)
22. Mansuripur, M.: J. Appl. Phys. **61**, 1580 (1987)
23. Deviren, B., Ertaş, M., Keskin, M.: Physica A **389**, 2036 (2010)
24. Deviren, B., Sener, Y.: J. Magn. Magn. Mater. **386**, 12 (2015)
25. Feraoun, A., Zaim, A., Keroad, M.: Physica B **445**, 74 (2014)
26. Kodana, R.H.: J. Magn. Magn. Mater **200**, 359 (1999)
27. Vasilakaki, M., Trohidou, K.N.: Phys. Rev. B **79**, 144402 (2009)
28. El Hamri, M., Bouhou, S., Essaoudi, I., Ainane, A., Abuja, R., Dujardin, F.: J. Phys. Conf. Series **758**, 012023 (2016)
29. Metropolis, N.C., Rosenbluth, A.W., Rosenbluth, M.N., Teller, E.: J. Chem. Phys. **21**, 1087 (1953)
30. Essaoudi, I., Bärner, K., Ainane, A., Saber, M.: Physica A **385**, 208 (2007)
31. Bati, M., Ertaş, M.: Phas. Trans. https://doi.org/10.1080/01411594.2016.1277222 (2017)
32. Six, L., Ieng, S., Saunier, J., Guessoum, Z.: https://hal.archives-ouvertes.fr/hal-00749726
33. Deviren, B., Keskin, M., Canko, O.: Physica A **388**, 1835 (2009)
34. Chakrabarti, K., Acharyya, M.: Rev. Mod. Phys. **71**, 847 (1999)
35. Essaoudi, I., Bärner, K., Ainane, A., Saber, M.: Phys. Scr. **75**, 500 (2007)
36. Saber, M.: Chin. J. Phys. **35**, 577 (1997)
37. Bati, M., Ertaş, M.: J. Supercond. Nov. Magn., https://doi.org/10.1007/s10948-016-3620-1
38. Fiorani, D.: Surface Effects in Magnetic Nanoparticles. Springer Science + Business Media, New-York (2005)
39. Bati, M., Ertas, M.: Superlattices Microstruct. **98**, 259 (2016)